Proceedings of ICAPP '08
Anaheim, CA USA, June 8-12, 2008
Paper 8288

NaK Plugging Meter Design for the Feasibility Test Loops

J Boise Pearson, Thomas J. Godfroy, Robert S. Reid, Kurt A. Polzin
NASA Marshall Space Flight Center, Huntsville, AL
256-961-0078 , 256-544-5926 , J.Boise.Pearson@nasa.gov

Abstract – *The design and predicted performance of a plugging meter for use in the measurement of NaK impurity levels are presented. The plugging meter is incorporated into a Feasibility Test Loop (FTL), which is a small pumped-NaK loop designed to enable the rapid, small-scale evaluation of techniques such as in situ purification methods and to permit the measurement of bulk material transport effects (not mechanisms) under flow conditions that are representative of a fission surface power reactor. The FTL operates at temperatures similar to those found in a reactor, with a maximum hot side temperature of 900 K and a corresponding cold side temperature of 860 K. In the plugging meter a low flow rate bypass loop is cooled until various impurities (primarily oxides) precipitate out of solution. The temperatures at which these impurities precipitate are indicative of the level of impurities in the NaK. The precipitates incrementally plug a small orifice in the bypass loop, which is detected by monitoring changes in the liquid metal flow rate.*

I. INTRODUCTION

The Early Flight Fission – Test Facility (EFF-TF) was established by the Marshall Space Flight Center to provide a capability for performing hardware-directed activities to support multiple in-space nuclear reactor concepts by using a non-nuclear test methodology.[1,2] This includes fabrication and testing at both the module/component level and near prototypic reactor configurations allowing for realistic thermal-hydraulic evaluations of systems. The EFF-TF is currently supporting an effort to develop an affordable fission surface power (AFSP) system that could be deployed on the Lunar surface.[3] Through a strong partnership with the Los Alamos National Laboratory (LANL), facets of conceptual reactor designs are translated into non-nuclear tests of hardware at NASA Marshall Space Flight Center. The AFSP system is presently based on a pumped liquid metal-cooled reactor design.[4,5] This design was derived from the only fission system that the United States has deployed for space operation, the Systems for Nuclear Auxiliary Power (SNAP) 10A reactor, which was launched in 1965.[6] An important aspect of the current hardware development effort is the information and insight that can be gained from experiments performed in a relevant environment using realistic materials. This testing can often deliver valuable data and insights with a confidence that is not otherwise available or attainable.

Early reactor studies have identified uncertainty with respect to the rates of corrosion of stainless steel in the presence of a eutectic mixture of sodium and potassium, NaK78 in this case, at estimated operating conditions. In high temperature alkali metal systems the issue of corrosion is a major concern. Often it is difficult to assess or quantify the rates of corrosion because of a confluence of transport, corrosion, and chemical mechanism and interactions. Of specific interest is the rate of corrosion of 316L stainless steel and NaK at the "best estimate" operational conditions for a FSP system.[5]

Feasibility Test Loops (FTLs) will be used to remedy this lack of corrosion data. The FTLs are small pumped-liquid metal loops designed to assess and resolve potential issues that may be encountered in FSP systems that are cooled by either Na or NaK. The loops allow for rapid examination of issues such as corrosion and material transport, the effects of freezing and thawing a liquid-metal coolant in the loop, and coolant expansion and gas generation during loop operation. They are also designed to permit the evaluation of techniques to perform on-line NaK impurity measurement and purification.

The first loop, FTL-1, is being fabricated with capability to achieve temperatures, temperature differences, flow velocities, and length to diameter (L/D) ratios that are representative of a prototypical AFSP reactor system. The first in a series of FTL experiments, its initial goals are the testing of the on-line impurity measurement technique and the evaluation of the capability to perform NaK purification during loop operation.

II. FEASIBILITY TEST LOOP-1

The FTL-1 experiment requirements were developed to address the rates of corrosion in flow passages of the current "best estimate" reactor design. The Los Alamos National Laboratory reactor design requires the use of three distinct flow passage areas through the core to maintain desired heat removal, power distribution balance, and pressure drop. The differing area passages will facilitate core power flattening to enable increased operational lifetime of the reactor by mitigating stresses in the reactor. The experiment will be used to quantify corrosion rates of prototypic materials, in this case 316L stainless steel, by NaK flowing through different area passages at specified design temperatures, temperatures differences, pressure levels, and flow rates. The balance of the loop is designed to deliver these specified test conditions in a test section. Table 1 gives details regarding the core average design parameters used to guide the requirements for FTL-1.

TABLE 1

Core average properties used to guide the design of FTL-1

Parameter	Value	Units
Coolant	NaK eutectic	
Thermal Conductivity	25.95	$W\ m^{-1}K^{-1}$
Viscosity	1.599E-4	$kg\ m^{-1}\ s^{-1}$
Density	738.78	$kg\ m^{-3}$
Specific Heat	874.07	$J\ kg^{-1}\ K^{-1}$
Inlet Temperature	840	K
Exit Temperature	880	K
Nominal Pressure	140	kPa
Boundary Material	316L Stainless Steel	

The test loop consists of a closed ½" tube loop with a heated section, a hot test section, primary heat exchanger (HX), cold test section, flow through reservoir, electromagnetic (EM) pump, and primary flow meter. The plugging meter used to determine oxygen concentration is a side branch bled from the high pressure to the low pressure side of the EM pump. The overall layout for the system can be seen in Figure 1.

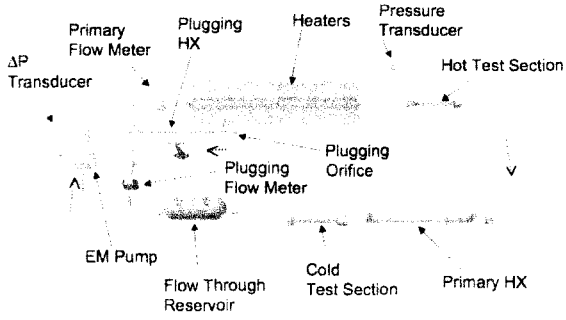

Figure 1. Physical layout of FTL-1

III. PLUGGING METER OVERALL DESCRIPTION

The plugging meter is an indicator of amount of solids precipitating out of solution with the NaK, in this case, Na_2O and K_2O. A side branch of the primary loop, the plugging meter loop is designed to draw a small portion of the flow from the pump. This sample flow is tested and returned to the low-pressure side of the pump.

The plugging meter loop consists of a small, well controlled heat exchanger to cool the NaK, a flow meter, and a small diameter screen to catch precipitates. The layout can be seen in Figure 1. As the heat exchanger gradually cools the NaK, the flow through the loop remains constant. When the loop has cooled to the level where the NaK is saturated with dissolved oxygen, any further reduction in temperature will result in precipitation of solid Na_2O and K_2O. These precipitates will start to plug the screen and inhibit flow, causing the flowrate to drop. The solubility of oxygen in NaK is well defined as a function of temperature, and can be used to determine the concentration of oxygen. Figure 2 shows the solubility of oxygen in NaK78 with temperature[7] along with a curve fit generated using the data.

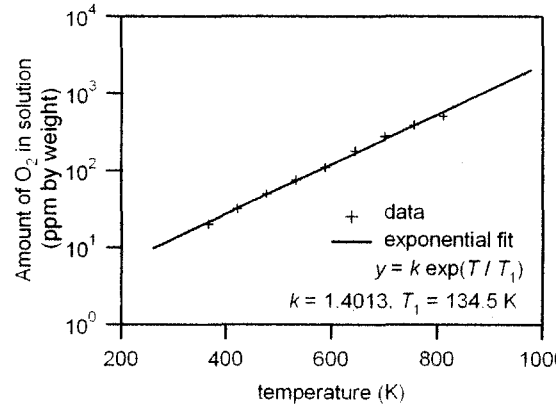

Figure 2. Amount of O_2 present in solution as Na_2O in NaK78 as a function of temperature.[7]

The temperature changes have to occur slowly, with both the forward and the reverse processes (i.e. precipitating the oxides and returning the precipitates into solution) being observed. Some hysteresis between the precipitation and reverse process has been observed,[8] and a combination of the two provides the most accurate measure of the temperature reflecting the oxygen concentration in the NaK. The details of sizing the orifice and flowmeter are crucial, and are detailed in later sections.

IV. PLUGGING HEAT EXCHANGER

Figure 3 shows a cross section of the plugging heat exchanger design. Gaseous nitrogen is used to remove the

heat in an open cycle system. The NaK enters at 880 K and exits at as low as 273 K. Bellows are utilized to accommodate the thermal dissimilarity and resultant expansion differences between the NaK tube and the nitrogen barrier. Stainless steel VCR fittings (not depicted) are used to mate with other loop components. A mass flow controller is located upstream of the heat exchanger and controls the flow rate of the nitrogen gas to automatically adjust and maintain required temperature differentials. The same design is used for both the primary heat exchanger and the plugging meter heat exchanger, with the main differences being the tubing diameters (1/2" vs. 1/4") and the length of the bellows sections.

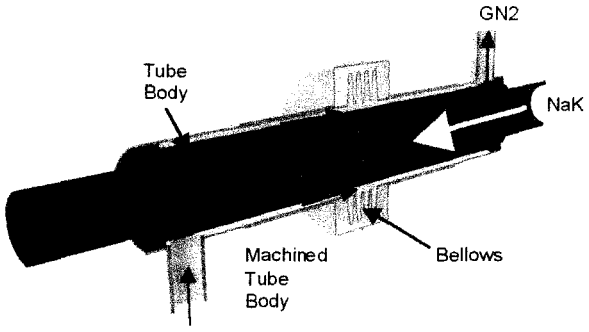

Figure 3. Plugging heat exchanger cross section, with bellows section shown shortened for simplicity.

V. PLUGGING FLOW METER

There are two flow meters in the FTL-1, one in the primary loop and one in the plugging loop. Both operate on the same principle and have the same basic conceptual design, but differ in the amount of flow they are designed to measure. The plugging flow meter does not need to be calibrated, as it is measuring relative changes in flow (from unplugged through plugged) rather than an absolute flow rate value.

V.A. Flow Sensor Theory of Operation

A DC electromagnetic (EM) flow sensor is implemented into the plugging loop to monitor the change in flow rate as oxides precipitate out of the NaK solution and block the plugging meter holes. An idealized schematic of a DC EM flow sensor is presented in Figure 4. The liquid metal flows though a channel of width w, length l, and height s. The magnetic field B and time-varying flow rate $u(t)$ are perpendicular both to each other and the direction across which the voltage $v(t)$ is measured. When an electrically conductive medium (a conducting liquid in this case) moves transverse to an applied field, a back-EMF is induced according to the vector equation

$$\vec{E} = -\vec{u} \times \vec{B} \ . \qquad (1)$$

Integrating the electric field over the width w (assuming spatially uniform values of u and B over the indicated faces), the voltage induced across the channel for a given mass flow rate, or the corresponding volumetric flow rate, is equal to

$$v = \frac{\dot{m}B}{\rho s} = \dot{V}\frac{B}{s} \ . \qquad (2)$$

The voltage output by the flow sensor is linearly dependent on the ratio B/s, making even an absolute measurement relatively simple once the meter has been calibrated.

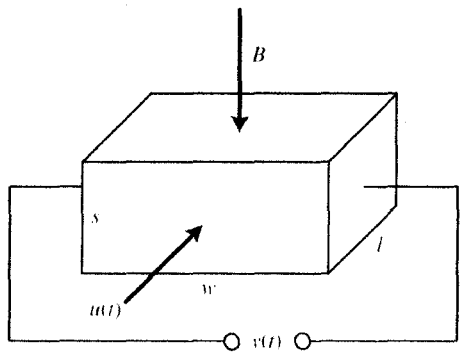

Figure 4. Electromagnetic flow sensor schematic

V.B. Sensor Design

From Equation (2) we observe that the flow sensor's voltage output for a given flow rate is increased with an increasing value of B/s. Consequently, this ratio was maximized in the design of the plugging loop flow sensor to yield high sensitivity.

Renderings of the flow sensor are shown in Figure 5. The hot liquid NaK is conducted through a 0.16 cm (1/16 in) diameter stainless steel tube. Two permanent neodymium rare-Earth magnets are located on each side of the tube, imposing an applied field in the vertical direction. The neodymium magnets have a relatively low Curie temperature (80-100 °C), so they are held a small distance away from the flattened tube, which has a temperature of up to 900 K. The resulting vacuum gap allows only radiative heat transfer from the steel to the magnet face. The water-cooled copper blocks serve to conductively transfer heat from the magnets. In addition, they also provide the structure required to keep the magnets a given distance apart from each other. The magnetic circuit is completed using FluxTrol, which is a magnetically permeable material. Thin metal weld rods (electrodes) are

attached to the sides of the tube to permit measurement of the transverse, induced voltage. The magnets are much wider than the tube and much longer than the electrodes in the direction of fluid flow to keep the field strength relatively constant over the measurement region.

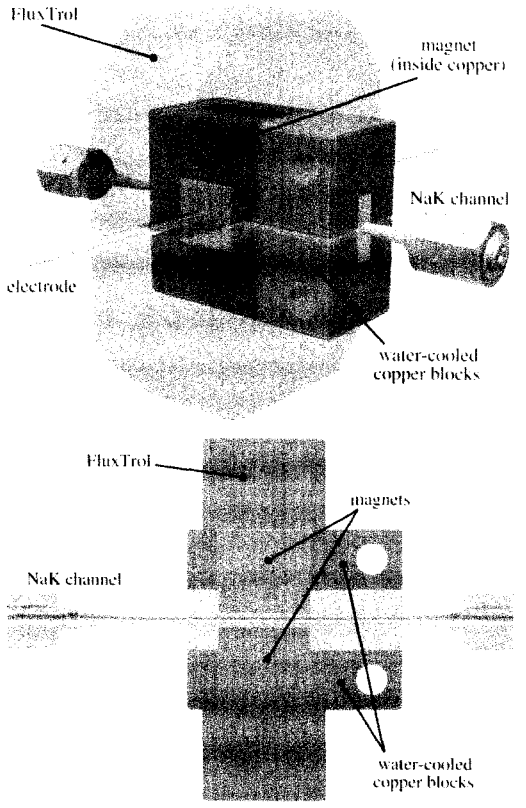

Figure 5. Renderings of the EM flow sensor design. Upper panel shows an oblique view with FluxTrol rendered transparent to reveal inner detail. Lower panel gives a cross sectional view.

V.C. Estimated Performance

The magnetic field is found using a two-dimensional magnetostatic solver package (Quickfield). This solver has the capability of modeling materials, like the FluxTrol and the neodymium magnets, which possess non-linear *B-H* characteristics. The *B-H* curves for each material in the vertical direction (orientation as shown in Figure 5) are given in Figure 6, where *H* is the magnetic intensity. A solution from the magnetostatic model is presented in Figure 7. The average value of *B* inside the NaK channel is calculated as ~1.07 T.

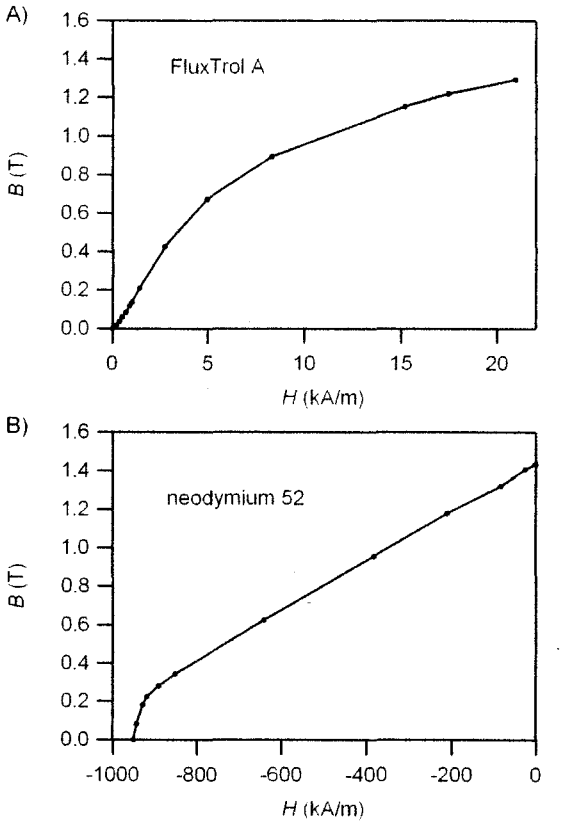

Figure 6. B-H characteristics for materials comprising the EM flow sensor magnetic circuit.

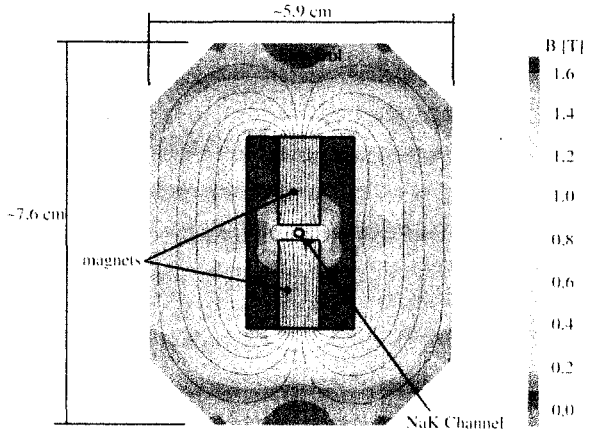

Figure 7. Magnetostatic simulation result for the geometry shown in Figure 5.

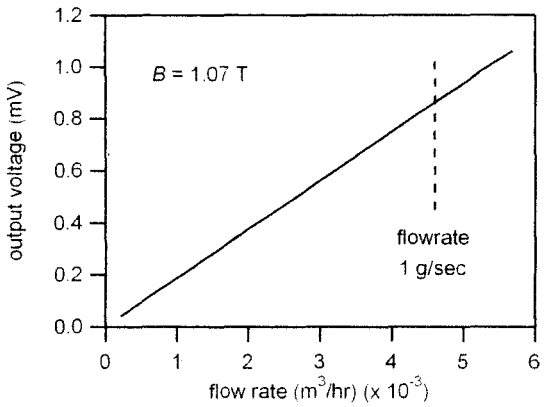

Figure 8. Estimated sensor output calculated using Equation (2).

The estimated output of the flow meter as a function of volumetric flow rate (throughput) is presented in Figure 8. The voltage output given by Equation (2) is linear with flow rate. In addition, the nominal flow rate expected in the flow sensor is about 1 g s^{-1}, corresponding to an output voltage just above 0.9 mV. This signal will be electronically amplified by a factor of ~10,000 to obtain higher resolution on the flow rate measurement.

VI. ORIFICE PLUGGING MECHANICS

Figure 9 shows one idealized orifice passage out of a close-packed circular array in the plugging meter. Each passage in the array has radius r and length L. An eutectic mixture of NaK, bearing non-metallic impurities at an unknown level, flows through the orifice. The orifice is cooled until there is a measurable decrease in mass flow rate from blockage by precipitating non-metallic impurities, here taken to be oxide.

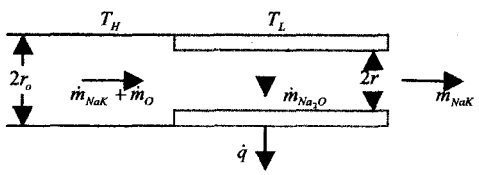

Figure 9. Idealized orifice passage used for sizing of holes in the plugging meter.

The molar balance for the NaK flowing through the system is

$$NaK + \frac{x}{2}[O] + y[O] \rightarrow (1-x)NaK + \frac{x}{2}Na_2O + x[K] + y[O], \quad (3)$$

where $x/2$ is the amount of oxygen precipitated from the NaK and y is the oxygen remaining in the NaK at saturation solubility. The precipitation rate from flowing NaK is

$$\dot{m}_p = (C_O - C_{Sol})\frac{M_p}{M_{NaK}}\dot{m}_{NaK}, \quad (4)$$

where C_O is the concentration of oxygen in the NaK, and C_{Sol} is the maximum possible concentration of oxygen in NaK having a temperature dependence of the form $C_{Sol} = ke^{T/T_1}$ from Figure 2. Precipitate grows on the orifice perimeter with mass

$$m_p = \rho_p n\pi L(r_o^2 - r^2). \quad (5)$$

The rate of change of film mass is

$$\dot{m}_p = -\rho_p n\pi L\frac{d(r^2)}{dt}. \quad (6)$$

The mass flow rate of NaK through n orifices having radius, r, is assumed to be laminar, giving

$$\dot{m}_{NaK} = n\frac{\Delta p\pi r^4}{16Lv}. \quad (7)$$

Combining Equations (4), (6), and (7) yields the differential equation

$$\frac{d(r^2)}{dt} + \frac{\Delta p(C_O - C_{Sol})}{16L^2v\rho_p}\frac{M_p}{M_{NaK}}r^4 = 0 \quad (8)$$

with initial condition $r = r_o$ at $t = 0$. This first-order, non-linear, homogeneous equation is satisfied by the Bernoulli form, with solution

$$r(t) = (\xi t + r_o^{-2})^{-0.5}, \quad (9)$$

where

$$\xi = \frac{\Delta p(C_O - C_{Sol})}{16L^2v\rho_p}\frac{M_p}{M_{NaK}}. \quad (10)$$

The nominal plugging meter loop values used in the sizing of the orifice are given in Table 2. The effect of changing orifice diameter on the mass flow rate through the plugging loop is presented in Figure 10.

TABLE 2

Nominal plugging meter values used in the sizing of the orifice

Parameter	Value	Units
C_o	1.30E-05	kg kg^{-1}
T	293	K
C_{Sol}	1.24E-05	kg kg^{-1}
Δp	3.45E+04	Pa
L	2.54E-03	m
d_o	1.00E-04	m
ν	5.00E-07	m^2 s^{-1}
ρ_p	2270	kg m^{-3}
n_p	3.7E+04	mol m^{-3}
M_p	62	-
M_{NaK}	33.82	-
ξ	8.46E+04	s^{-1} m^{-2}

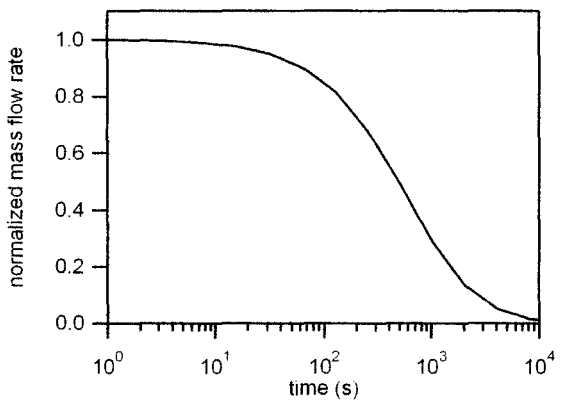

Figure 10. Normalized mass flow rate thru orifice versus time.

VII. ORIFICE DESIGN AND SELECTION

One final design constraint must be mentioned. The measurement must not appreciably change the measured quantity. In this case, sizing the system to handle a large range of oxygen concentrations makes it possible to remove enough oxygen from solution to easily violate that constraint without careful consideration. To avoid affecting the results, compare the volume of precipitates available as dissolved oxygen in the *entire system* V_V, to the volume of precipitates needed to fully plug the orifice V_P. The integrity of the results should be maintained when $V_P << V_V$, which has been limited for this case to be $V_P = 0.01 V_V$. This leads to the following relationship,

$$100 V_P \le V_V = \frac{C_O m_{NaK}}{M_{NaK} n_p}, \tag{11}$$

where m_{NaK} is the mass of NaK in the entire system and n_p is the molar density (mol m^{-3}) of the precipitate. For an overall orifice consisting of n identical smaller holes of diameter d_o and length L, a relationship can be determined for the volume V_P, and replaced in Equation (11) to create the following relationship:

$$100 \frac{n \pi d_o^2 L}{4} \le \frac{C_O m_{NaK}}{M_{NaK} n_p} \tag{12}$$

which can be rearranged to find a relationship between n and d_o

$$n \le \frac{C_O m_{NaK}}{25 M_{NaK} n_p \pi d_o^2 L}. \tag{13}$$

Equation (13) constrains the orifice based on the maximum allowable precipitate volume. Note that this is a function of oxygen concentration. Performing the measurement over two orders of magnitude while maintaining sensitivity over that range is one of the biggest challenges faced in implementing this plugging meter.

The final orifice design and sizing is a compromise between uncertainties in the analysis and the realities of manufacturing. The orifice itself is made from a Swagelok VCR seal blank with the center reduced to 0.015 in (3.8×10^{-4} m) thickness. The holes are laser drilled with a diameter of 0.0042 in (10^{-4} m). This manufacturing constraint defines the hole size and length, and leaves the number of holes as the major variable remaining. The number of holes through the blank as a function of mass flow rate and hole diameter are presented in Figure 11. The family of curves in the parameter space is defined by Equation (7) while the inequality in Equation (13) restricts the design space available.

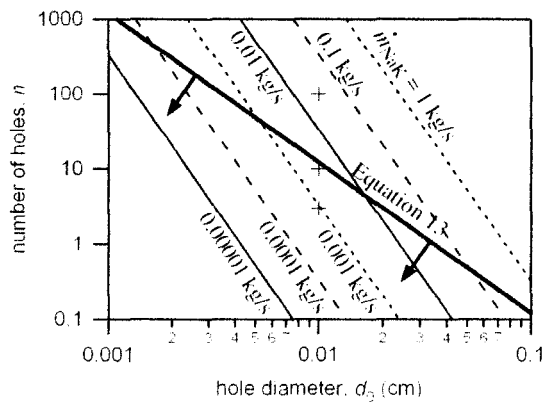

Figure 11. Number of holes through VCR gasket vs. diameter of holes and mass flow rate of NaK through the gasket. The arrows indicate the direction in which the inequality in Equation (13) is satisfied.

Three different VCR blanks were manufactured, one with three holes, one with ten holes and one with one hundred holes (all with diameters of 10^{-2} cm). Those three points are denoted by crosses on the 0.01 cm line in the trade space as shown in Figure 11. The middle cross represents 10 holes, and approximately 5 g s^{-1} of NaK flow through the orifice. The results in Figure 8 indicate that this is approximately 5 mV of signal from the flow meter. Imagining that the uncertainties in analysis and vagaries of hardware add up to an order of magnitude shift in result, the range of possible voltage outputs is still detectable.

IV. CONCLUSIONS

The FTL-1 is a pumped NaK loop designed to simulate relevant flow conditions in a FSP reactor. Several components have been developed to implement a plugging meter to determine oxygen concentration in the FTL-1. The unique flowmeter design allows high temperature operation of a liquid metal flowmeter with a designed output of ~ 0.8 mV g^{-1} s^{-1}. The plugging orifice was carefully designed to plug in a reasonable amount of time and not affect the oxygen concentration in the loop.

ACKNOWLEDGMENTS

This work was done with support of the Fission Surface Power program under NASA's Exploration Technology Development Program.

NOMENCLATURE

B, $\vec{B}$	magnetic field (T)
C_O	concentration of oxygen (ppm, by weight)
C_{Sol}	concentration of oxygen at saturation (ppm by weight)
d_o	diameter of plugging orifice (m)
$\vec{E}$	electric field (V m^{-1})
H	magnetic intensity (A m^{-1})
K	potassium
l	channel length (m)
L	plugging orifice length (m)
m	mass (kg)
m_p	mass of precipitate (kg)
m_{NaK}	total mass of NaK in FTL (kg)
m_p	mass of precipitate (kg)
$\dot{m}$	mass flow rate (kg s^{-1})
$\dot{m}_{NaK}$	NaK mass flow rate through orifice (kg s^{-1})
$\dot{m}_p$	oxide mass precipitation rate (kg s^{-1})
M_{NaK}	molecular weight of NaK (kg $kmol^{-1}$)
M_P	molecular weight of precipitate (kg $kmol^{-1}$)
n	number of orifices in plugging filter
n_p	molar density of precipitate (mol m^{-3})
Na	sodium
NaK	sodium potassium eutectic
O	oxygen
p	pressure (Pa)
r_o	plugging orifice radius (m)
r	changing orifice radius (m)
s	channel height (m)
t	time (s)
T	temperature (K, °C)
u, $u(t)$	flow rate (m s^{-1})
v, $v(t)$	voltage (V)
$\dot{V}$	volume flow rate (m^3 s^{-1})
V_V	volume of precipitate if all oxygen in system precipitates out (m^3)
V_P	total volume of plugging filter (m^3)
w	channel width (m)
ν	kinematic viscosity (m^2 s^{-1})
ρ	density (kg m^{-3})
ρ_p	density of precipitate (kg m^{-3})

REFERENCES

1. T. J. GODFROY, M. VAN DYKE, and R. DICKENS, "Realistic Development and Testing of Fission Systems at a Non-Nuclear Testing Facility," Space Technologies and Applications International Forum (STAIF-2000), AIP, **504**:1208 (2000).

2. M. VAN DYKE, T. J. GODFROY, M. HOUTS et al., "Results of a First Generation Least Expensive Approach to Fission Module Tests: Non-Nuclear Testing of a Fission System," Space Technologies and Applications International Forum (STAIF-2000), AIP, **504**:1211 (2000).

3. M. HOUTS, S. GADDIS, R. PORTER et al., "Options for Affordable Fission Surface Power Systems," Proceedings of the 2006 International Congress on Advances in Power Plants (ICAPP), ANS, paper 6370 (2006).

4. D. D. DIXON, M. HIATT, D. I. POSTON et al., "Design of a 25-kWe Surface Reactor System Based on SNAP Reactor Technologies," Space Technology and Applications International Forum (STAIF-2006), AIP, **813**:932 (2006).

5. D. I. POSTON, R. J. KAPERNICK, D. D. DIXON et al., "Reference Reactor Module for the Affordable Fission Surface Power System," Space Technology and Applications International Forum (STAIF-2008), AIP, **969**:277 (2008).

6. J. A. ANGELO and D. BUDEN, *Space Nuclear Power*. Orbit Book Company, Malabar, FL (1985).

7. R. N. LYON, *Liquid-Metals Handbook*. Atomic Energy Commission, Oak Ridge (1952).

8. J. W. MAUSTELLER, F. TEPPER, and S. J. RODGERS, *Alkali Metal Handling and Systems Operating Techniques*. Gordon and Breach, New York (1967).